Volume 17
Number 39
21 October 2021
Pages 8761–8984

Soft Matter

rsc.li/soft-matter-journal

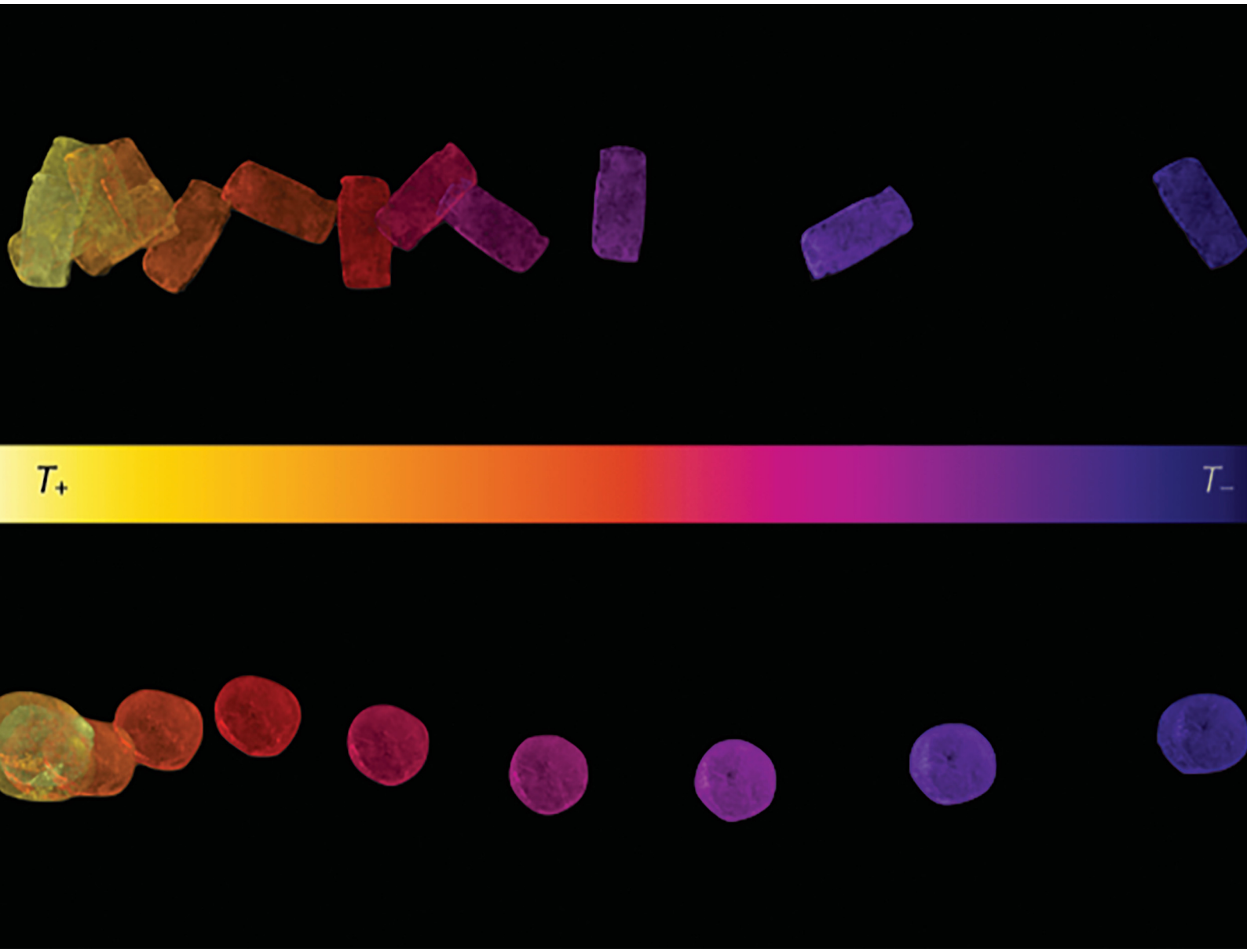

ISSN 1744-6848

ROYAL SOCIETY OF CHEMISTRY

PAPER
Ambre Bouillant *et al.*
Thermophobic Leidenfrost

Soft Matter

PAPER

View Article Online
View Journal | View Issue

Cite this: *Soft Matter*, 2021, 17, 8805

Thermophobic Leidenfrost†

Ambre Bouillant,[ab] Baptiste Lafoux,[ab] Christophe Clanet[ab] and David Quéré[ab]

Received 14th April 2021,
Accepted 19th June 2021

DOI: 10.1039/d1sm00548k

rsc.li/soft-matter-journal

We report that a volatile liquid deposited on a hot substrate with a gradient of temperature does not only levitate (Leidenfrost effect), but also spontaneously accelerates to the cold. This thermophobic effect is also observed with sublimating solids, and we attribute it to the ability of temperature differences to tilt (slightly) the base of the "object", which induces a horizontal component to the levitating force. This scenario is tested by varying the drop size (with which the acceleration increases) and the substrate temperature (with which the acceleration decreases), showing that the effect can be used to control, guide and possibly trap the elusive Leidenfrost drops.

The Leidenfrost phenomenon occurs when placing a volatile liquid on a hot plate. If the plate is brought above the so-called Leidenfrost temperature T_L (typically 170 °C for water), drops then levitate on a cushion of their own vapor,[1] which impedes boiling and insulates the liquid. The absence of contact between the liquid and its substrate shapes drops in non-wetting states,[2,3] either quasi-spherical at small radius R or flattened by gravity when R is large. The cross-over between these two regimes takes place around the capillary length $\kappa^{-1} = (\gamma/\rho g)^{1/2}$ (2.5 mm for water at 100 °C), where we denote γ and ρ as the liquid surface tension and density, and g as the acceleration of gravity. In a levitating situation, friction is especially low and these spheroids are extremely mobile, paving the way to rich and unusual dynamics. For instance, large puddles of liquid ($R > 4\kappa^{-1}$) are pierced by chimneys that periodically collapse and reform;[2] smaller puddles suddenly start to pulsate, with various star-modes;[4] millimetric spherical drops spontaneously self-propel in random directions,[5] until they take off when they reach submillimetric scales.[6,7]

The control of these elusive liquids concerns many applications, such as heat pipes and spray cooling. To that end, various strategies have been developed in the past decades. Linke *et al.* found that Leidenfrost drops placed on ratchets self-propel in a preferential direction.[8] Leidenfrost solids – dry ice platelets that sublimate at −79 °C – exhibit a similar behavior,[9] suggesting that propulsion arises from the rectification of the vapor flow below the levitating object, which draws it in a preferential direction – or even immobilizes it when the patterns are purposely designed.[10,11] In addition, sculpting dry ice in an asymmetric fashion can tilt its base, which yields a horizonal component of the lifting force, and thus propulsion.[12]

We herein discuss the possibility of conveying directional motion to Leidenfrost objects on a flat substrate by setting a gradient of temperature along the substrate (thermophoresis). It is well-known that a thermal Marangoni effect can drive drops along heterogeneously heated solids.[13–15] However, our situation is more challenging, owing to the absence of solid/liquid contact and to the implicit isothermal condition at the evaporating interface. Sobac *et al.* recently discussed the effect of temperature differences below a Leidenfrost drop and distinguished various possible effects.[16] On the one hand, the evaporation rate of the liquid depends on the substrate temperature, so that inhomogeneous heat may incline the drop base and induce propulsion toward cold – as observed in connected situations with lubricated layers.[5,12] On the other hand, the vapor properties (thermal conductivity, density, viscosity) may vary along the vapor film, which can also favor motion, yet possibly toward hot.[16] On the whole, neither the existence nor the direction (and intensity) of propulsion can be easily deduced from the calculations, which stimulates an experiment on this topic.

The principle of our experiment is sketched in Fig. 1a. The substrate consists in a bar of brass (length $L \approx 22$ cm, width of 4 cm) micromachined to display an axial shallow parabolic gutter (central depth 0.5 mm), which restricts drops motion to the gutter x-axis (see details in the ESI†). The bar extremities contact two heaters, which imposes $T_+ \approx 350$ °C at $x = 0$ and $T_- = T_+ - \Delta T \approx 150$ °C at $x = L$. Heat exchanges within the solid being dominated by diffusion, the temperature $T(x)$ varies linearly along the substrate, with a uniform gradient $|G| = \Delta T/L \approx 7$–$10$ °C cm^{-1}. The transient and permanent heating regimes are characterized by an infra-red camera, as

[a] *Physique & Mécanique des Milieux Hétérogènes, UMR 7636 du CNRS, ESPCI, 75005 Paris, France*
[b] *LadHyX, UMR 7646 du CNRS, École polytechnique, 91128 Palaiseau, France*

† Electronic supplementary information (ESI) available. See DOI: 10.1039/d1sm00548k

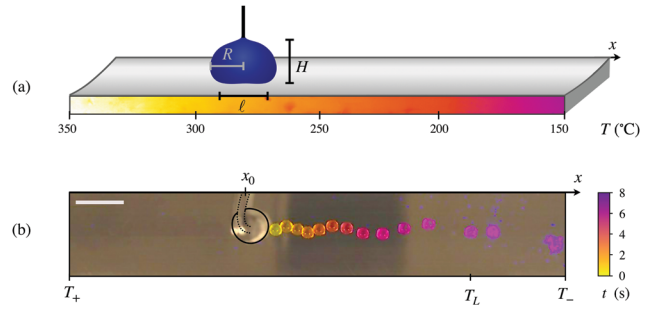

Fig. 1 Behavior of a Leidenfrost drop on a thermal gradient. (a) Schematic of the experiment: a brass bar (length L = 22 cm) slightly curved in the direction perpendicular to its main axis x is heated differentially. The temperature is T_+ on the left and T_- on the right, resulting in a thermal gradient G of typically −10 °C cm^{-1}. We follow water drops with radius R dispensed from a needle at a position x_0 and height H after they detach from the needle, owing to evaporation. Their bases with diameter ℓ experience a mean temperature $T(x_0)$ and a temperature difference $G\ell$. (b) Top-view chronophotography showing a water drop with R = 2.6 mm starting at x_0 = 8 cm on a plate with gradient $G \approx -9$ °C cm^{-1}. Interval between successive photos is 0.4 s and colors are used to better distinguish them. The drop spontaneously accelerates toward the cold side. When it reaches the position x_L such that $T(x_L) \approx T_L$, it suddenly boils, as shown by non-circular shapes and fragments. The dispensing system is framed in black, the bar indicates 2 cm and the corresponding movie is Movie 2 (ESI†).

detailed in the ESI.† Airflows above the heated bar are directed upward with a typical velocity of 20 cm s^{-1}, as revealed by tracers (see Movie 1, ESI†); yet, we do not observe any measurable horizontal airdrift likely to entrain the levitating drop.

A water drop with equatorial radius $R \approx 2.6 \pm 0.2$ mm is dispensed from a needle located at $x_0 \approx 8$ cm and ending at a height $H \approx 3.6 \pm 0.4$ mm above the substrate having a temperature gradient $G \approx -9$ °C cm^{-1}. The drop base of diameter $\ell \approx 3.5 \pm 0.4$ mm initially faces a mean temperature $T_0 = T(x_0) \approx 285$ °C and a temperature difference $G\ell \approx 3$ °C. The evaporating liquid shrinks until it its height compares with H, so that it detaches from the needle: this technique enables us to control the initial radius $R(H)$ of the drop and to minimize the initial velocity of water. We record the experiment with a top-view video-camera and the chronophotography in Fig. 1b (see also Movie 2, ESI†) shows the successive positions of the drop separated by 0.4 s and distinguished by colors.

Water is observed to leave its initial position and to accelerate to the cold. It reaches velocities as high as a few centimeters per second, up to the point where it crosses the position x_L defined by $T(x_L) = T_L$, at which it suddenly boils – as revealed by small fragments emitted by the drop, its non-circular shape and its perturbed trajectory. As it moves, water slightly gets off centered, but the curvature of the substrate brings it back to the main axis, keeping trajectories roughly unidirectional. The gutter is important to that end: drops deposited on flat bars generally flee to the lateral sides of the bar (from which they escape), a consequence of a smaller temperature of these sides exposed to ambient air. Hence, all experiments were performed with a gutter, allowing us to follow long range motions.

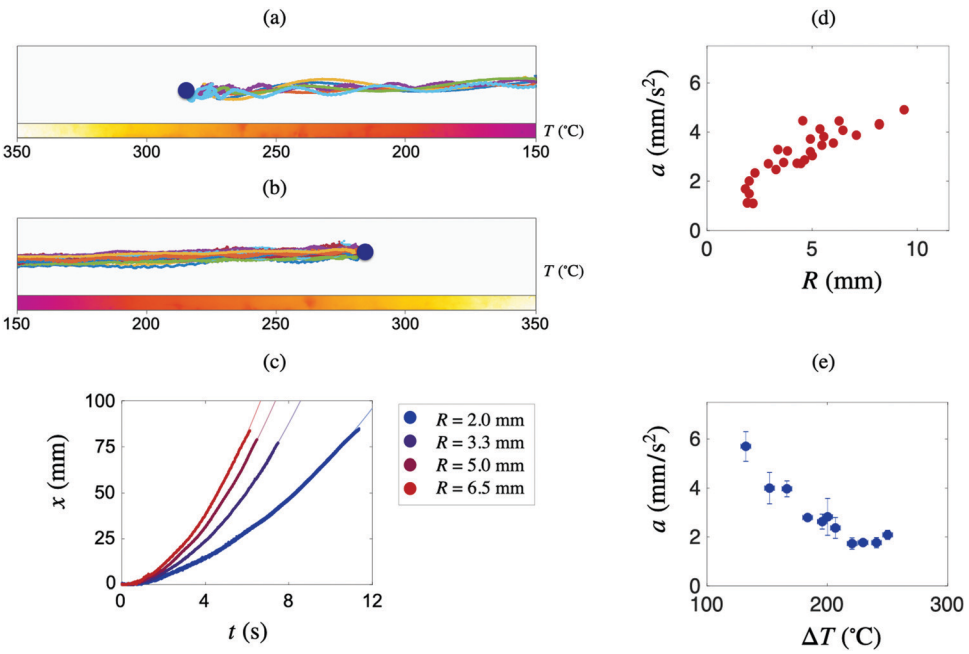

Fig. 2 Thermophobic Leidenfrost effect. (a) Superimposition of twenty top-viewed trajectories of water drops with radius R = 2.6 ± 0.1 mm. The substrate temperature $T(x)$ varies as Gx, with G = −8 °C cm^{-1}. Drops released at $x = x_0$, where the substrate temperature T_0 is 285 °C (blue dot), all self-propel toward the cold with almost straight-lined trajectories. (b) If the same experiment is performed with G = +8 °C cm^{-1}, trajectories are inverted. (c) Drop position x as a function of time t for different radii R. Data are obtained with $|G|$ = 8 °C cm^{-1} and trajectories are fitted by quadratic functions $x(t) = a(t - t_0)^2/2$ (thin solid lines), t_0 being the detachment time. We deduce from each fit the drop acceleration a. (d and e) Acceleration a as a function of the drop radius R (at fixed T_0 = 285 ± 3 °C) and as a function of $\Delta T = T_0 - T_b$ (at fixed R = 4.6 ± 0.2 mm), denoting T_b as the water boiling point.

To go further in the analysis, we repeat the experiment and record the liquid paths. Fig. 2a collects the trajectories of twenty drops (R = 2.6 ± 0.2 mm) placed on a gradient $G = -8$ °C cm^{-1}. As evidenced by the use of distinctive colors for each experiment, all drops starting from rest systematically moves toward the cold. However, even tiny slopes could guide the levitating Leidenfrost drops and horizontality of the substrate along x was first adjusted with a highly-sensitive spirit level with a precision $\alpha_o < 0.1$ mrad. The corresponding gravity acceleration $\alpha_o g$ is at most 1 mm s^{-2}, smaller than 4 mm s^{-2}, the typical acceleration deduced from the trajectories. We confirmed that gravity was not the cause of the observed movement by inverting the temperature gradient on a given bar. As seen in Fig. 2b, the motion is inverted the same way (see the ESI† for complements related to the thermal expansion of the substrate), confirming the existence of a thermophoretic force, which we now try to characterize and understand.

The duration of an experiment is less than 10 s, much shorter than the few minutes for evaporating the liquid, so that we can neglect the radius variation in our experiment. We report it in Fig. 2c the position $x(t)$ of drops with radii R ranging from 2 mm to 10 mm, the largest explorable interval. As discussed in the ESI,† smaller drops are subjected to an isotropic self-propulsion even in the absence of thermal gradient,[5] while bigger ones are pierced by a central chimney of vapor that significantly affects their geometry.[2] Looking at the four trajectories reported in Fig. 2c, we first notice that the larger the drops, the faster they are: the time needed to travel by 7 cm is increased by about 50% when R roughly triples. All data can be fitted by quadratic functions drawn with thin solid lines, $x(t) = a(t - t_0)^2/2$, denoting a as the drop acceleration and t_0 as the detachment time. The fitting parameter t_0 in Fig. 2c is between 0.2 and 1.1 s, a value that reveals the uncertainty on the detachment time and the delay required to dissipate vertical bouncing caused by detachment before drops start to move.

Hence, in first approximation, the drop acceleration a is constant during a run. In Fig. 2d, we show how it varies with the radius R at fixed initial temperature $T_0 = T(x_0) = 285 \pm 3$ °C: a indeed increases with R, which attests that gravity (either arising from unavoidable deviations from horizontality or from the thermal expansion of the substrate) is not the main cause of the motion (in which case a would not depend on R), and suggests propulsion is more efficient for larger drops. The levitation height ε increases with the substrate temperature T and it is natural to test how the thermophobic effect is sensitive to this parameter, which we vary by placing drops at various initial locations x_0. Fig. 2e shows that the acceleration a (plotted as a function of $\Delta T = T_0 - T_b$) decreases with the temperature experienced at detachment: despite its thermal origin, the effect is enhanced on colder environments, that is, at smaller levitation heights.

We can also question the influence of the nature of the Leidenfrost object: liquid can host deformations, waves and Marangoni flows – the latter phenomenon being indeed responsible for the cold-directed motion of non-levitating drops on thermal gradients.[13–15] To turn these effects off, we consider sublimating carbon dioxide, a solid known to float in the Leidenfrost state above hot plates.[12] Following the protocol defined in Fig. 1a, we deposit disks or cubes of dry ice (with a diameter or size $\ell \approx 10 \pm 2$ mm, height $h \approx 10 \pm 2$ mm and mass m of a few grams) upon the inhomogeneously heated substrate. What happens for twenty platelets is shown in Fig. 3a for $G = -7$ °C cm^{-1}. Despite some disparity in their geometry, all pieces of ice leave their initial position and get propelled to the cold, like liquids and with a similar dynamics: 10 cm are travelled in typically five seconds, which implies an acceleration of a few mm s^{-2} (see the Section S5 of the ESI† for complements). The same thermophobic behavior is observed when the sign of the gradient is reversed ($G = +7$ °C cm^{-1}, Fig. 3b).

These additional experiments suggest that the movement is mainly caused by an asymmetry at the platelet base. As sketched in Fig. 3c, we assume that the side exposed at a temperature T_+ gets eroded more than the one at T_-, which results in a difference $\Delta\varepsilon = \varepsilon(T_+) - \varepsilon(T_-)$ of the vapor thickness below the platelet. The tilt at the object base gives birth to a horizontal component of the levitating force, which propels the platelet to the cold.[12]

More quantitatively, the vapor thickness ε results from a balance between incoming and outcoming gas flows. On the one hand, the heat flux per unit area can be written $\lambda\Delta T/\varepsilon$,

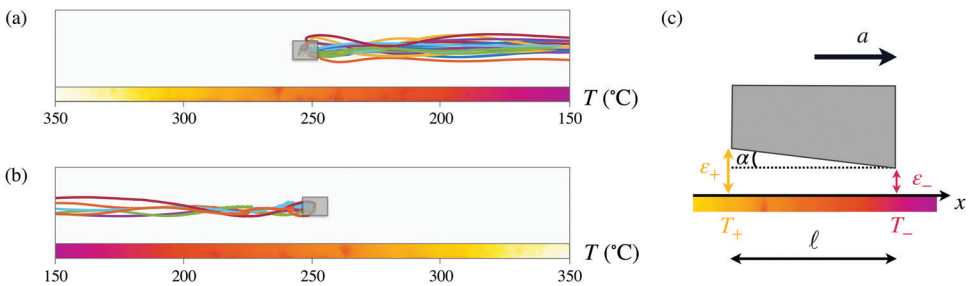

Fig. 3 Dry-ice thermophobia. (a) Superimposition of twenty trajectories of platelets of dry ice with mass m ranging from 1 to 10 g on a substrate with a gradient of temperature $G = -7$ °C cm^{-1} and $T_0 = 250$ °C. Each solid, initially at rest, self-propels toward the cooler end of the substrate with straight trajectories. (b) Same experiment after reverting the temperature gradient ($G = +7$ °C cm^{-1}). Leidenfrost solids consistently head toward the cold side of the bar. (c) Schematic of a platelet above a substrate with $G < 0$. Sublimation intensifies with temperature, which can induce an asymmetric erosion of the solid and tilt the ice base gets by an angle α. Such a tilt accelerates the ice by $a = \alpha g$ to the cold.

where λ is the thermal conductivity of the vapor, which leads to a production rate $\lambda\Delta T\ell^2/L\varepsilon$, with L the latent heat of sublimation. On the other hand, the gas (of density ρ_v and viscosity η_v) pressed by the platelet escapes at a Poiseuille rate $(\rho_v\varepsilon^3/\eta_v)\rho gh$. Balancing these two quantities provides a stationary thickness $\varepsilon \sim [\lambda\eta_v\Delta T\ell^2/\rho_v\rho ghL]^{1/4}$, in the range of 10 to 100 μm. ε increases with the substrate temperature, so that a temperature difference between both sides of the platelet can tilt its base: the relative variation of thickness scales as $G\ell/\Delta T$, which carves a tilt angle $\alpha \sim \Delta\varepsilon/\ell \sim G\varepsilon/\Delta T$. The horizontal component of the levitating force mg is $mg\alpha$, from which we deduce a platelet acceleration $a \approx \alpha g$ scaling as $Gg\varepsilon(\ell,\Delta T)/\Delta T$. For $G \approx 10$ °C cm^{-1}, $\varepsilon \approx 50$ μm and $\Delta T \approx 200$ °C, the latter quantity is a few mm s^{-2}, consistently with our observations.

Other quantities in the expression of ε depend on temperature, namely the vapor conductivity, viscosity and density: λ, η_v and $1/\rho_v$ all increase with T. Assuming that vapor adopts the local temperature of the substrate, the thermal gradient tends to tilt the platelet as previously, which just reinforces the effect.[16] As shown in the ESI,† the tilt angle deduced from deriving the function $\varepsilon(\lambda, \eta_v, \rho_v)$ with respect to T is, cumulatively, significantly weaker than the one generated by erosion, which we consider further as the main source of propulsion.

Drops with equatorial radius R comparable to the capillary length κ^{-1} are flattened by gravity as sketched in Fig. 4a. Owing to Archimedes thrust, they host a dimple at their base,[17] whose height is typically $0.02\kappa^{-1}$ for $R \sim \kappa^{-1}$,[2,3] which allows us to treat the base as flat and to directly exploit the model derived for a solid. The base extent ℓ scales as R and the liquid height h as κ^{-1}, which yields a film thickness $\varepsilon \sim [\lambda\eta_v\Delta TR^2/\rho_v\rho g\kappa^{-1}L]^{1/4}$. Hence the tilt of the base $\alpha \sim \Delta\varepsilon/R \sim G\varepsilon(R,\Delta T)/\Delta T$ is found to scale as $G[\lambda\eta_v/\rho_v\rho g\kappa^{-1}L]^{1/4}\ R^{1/2}/\Delta T^{3/4}$, which increases with the drop radius and decreases with the temperature substrate, as observed experimentally (Fig. 2c, d and e, respectively). Fig. 4b shows that the calculated angle α is indeed proportional to the measured acceleration a/g (the constant of proportionality being of order unity), with a collapse of the data in this representation, whatever their origin – either after varying the drop radius (red data) or the substrate temperature (blue data).

Despite this satisfactory agreement, we can discuss further the comparison between data and model. We first report in Fig. 4c the instantaneous velocity of a water drop (R = 6.5 mm, T_0 = 285 °C and G = −8 °C cm^{-1}) derived from its trajectory $x(t)$ (data from Fig. 2c). Apart from an initial regime where the drop detaches from the needle and transiently, albeit weakly, bounces, which delays the motion, the velocity is roughly linear in time – from which we can extract a mean acceleration $\langle a\rangle$, as shown earlier. We deduce from this curve the instantaneous acceleration $a(t)$, which we plot in Fig. 4d. After the already-mentioned transient regime (the first 0.75 second, before the vertical dotted line), a reaches ∼4 mm s^{-2}, a value that compares with that deduced from the fit in Fig. 2c and recalled by a red horizontal line in the figure. However, the acceleration still varies once this value is reached. (i) The main visible effect consists in oscillations (between ∼3 and ∼5 mm s^{-2}), which can be accounted for the existence of a y-component of the motion visible in the Fig. 2a, b and 3a, b. Trajectories are mainly along x but the acceleration along y is not strictly zero, so that drops oscillate in the direction perpendicular to the gutter with a period $\tau \approx 2\pi/(Cg)^{1/2}$, where C is the substrate curvature in the y-direction. As shown in the ESI,† the gutter profile is parabolic with a curvature ∼3 m^{-1}, which provides a period τ on the order of 1 second, in agreement with the observations. Owing to the frictionless nature of the motion, kinetic energies along x and y exchange and conserve, so that motion along y does not inhibit the effect reported in this note, namely a constant drift to the cold. (ii) The mean value of the acceleration $\langle a\rangle$ increases with time by about 20%, as shown by the linear fit of $\langle a(t)\rangle$ drawn with dots. We expect such an increase from the model: as drops move to the cold, the substrate temperature decreases by $\delta\Delta T$, which should induce a relative variation $\delta\alpha/\alpha = -\frac{3}{4}\,\delta\Delta T/\Delta T$ of the tilt. The quantity ΔT varies by typically 30% in an experiment, with an expected variation $\delta a/a = \delta\alpha/\alpha$ on the order of +20%. This qualitatively agrees with the observations: the thermophobic behavior is slightly reinforced as going to the cold (a counter-intuitive effect). This effect is modest, which legitimates the choice of a constant (average) acceleration along the drops trajectory.

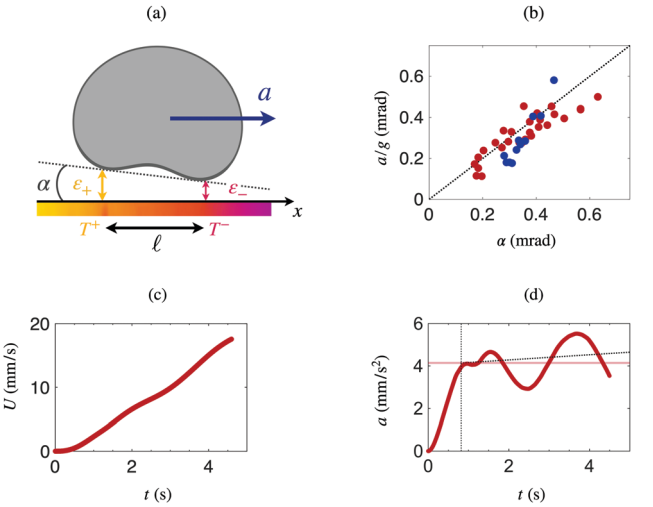

Fig. 4 Thermophobic dynamics of a Leidenfrost drop. (a) Sketch of a drop with radius R (comparable to the capillary length) having a base tilted by the temperature gradient. The horizontal component of the levitating force accelerates the drop to the cold. (b) Measured acceleration a, normalized by g, as a function of the base tilt α estimated from the model. We plot the two families of data shown in Fig. 2d and e, obtained by varying either the drop radius (red data) or the temperature T_0 (blue data). (c) Drop velocity U derived from the position $x(t)$ for R = 6.5 mm, T_0 = 285 °C and G = −8 °C cm^{-1} (trajectory reported in Fig. 2c). (d) Drop acceleration $a(t)$ derived from $U(t)$. After a short transient regime, the acceleration reaches a pseudo-plateau at $t \approx 0.75$ s, with $a \approx 4$ mm s^{-2} (red line). During the rest of the trajectory (more than 10 cm), a fluctuates and its mean value slowly increases, by about 20% (blue dotted line).

In summary, we reported that Leidenfrost drops placed on thermal gradients self-propel toward the cold, travelling by 15 cm in typically 5 to 10 s. This thermophobic behavior is also observed with Leidenfrost solids, suggesting that the liquid nature of drops is not essential in the propelling

mechanism; we rather assumed that motion relies on a tilt α of the base of the levitating object, whatever its nature. It would be interesting to extend these findings to radial geometries, considering a conductive disk and making it hot either at the center or at the periphery, which should generate either the radial expulsion of drops or their capture at the center, as observed with concentric ratchets.[10]

Even if the force driving the motion is a fraction of a microNewton, the ultra-low friction makes dynamics quick, with velocities on the order of 1 cm s^{-1}. In addition, the effect being sensitive to the substrate temperature itself (and not only to its gradient), it can be slightly amplified as the drop moves to the cold – and even, possibly, to its own end: if the substrate temperature crosses the Leidenfrost point as it does in Fig. 1b, drops reaching this frontier suddenly boil and split, being however inertially entrained beyond this "lethal" point. In order to extend the regime of smooth transportation of the drop, we might cover the substrate with a superhydrophobic coating – a recipe known to lower significantly the Leidenfrost point,[18] and thus expected to shift the place where drops explode.

Conflicts of interest

There are no conflicts to declare.

References

1 J. G. Leidenfrost, On the fixation of water in diverse fire, *Int. J. Heat Mass Transfer*, 1966, **9**(11), 1153–1166.
2 J. H. Snoeijer, P. Brunet and J. Eggers, Maximum size of drops levitated by an air cushion, *Phys. Rev. E: Stat., Nonlinear, Soft Matter Phys.*, 2009, **79**(3), 036307, DOI: 10.1103/PhysRevE.79.036307.
3 A.-L. Biance, C. Clanet and D. Quéré, Leidenfrost drops, *Phys. Fluids*, 2003, **15**(6), 1632–1637.
4 X. Ma, J.-J. Liétor-Santos and J. C. Burton, Star-shaped oscillations of Leidenfrost drops, *Phys. Rev. Fluids*, 2017, **2**(3), 031602, DOI: 10.1103/PhysRevFluids.2.031602.
5 A. Bouillant, T. Mouterde, P. Bourrianne, A. Lagarde, C. Clanet and D. Quéré, Leidenfrost wheels, *Nat. Phys.*, 2018, **14**, 1230.
6 F. Celestini, T. Frisch and Y. Pomeau, Take off of small Leidenfrost droplets, *Phys. Rev. Lett.*, 2012, **109**(3), 034501, DOI: 10.1103/PhysRevLett.109.034501.
7 S. Lyu, V. Mathai, Y. Wang, B. Sobac, P. Colinet, D. Lohse and C. Sun, Final fate of a Leidenfrost droplet: Explosion or takeoff, *Sci. Adv.*, 2019, **5**, eaav8081, DOI: 10.1126/sciadv.aav8081.
8 H. Linke, B. J. Alemán, L. D. Melling, M. J. Taormina, M. J. Francis, C. C. Dow-Hygelund, V. Narayanan, R. P. Taylor and A. Stout, Self-Propelled Leidenfrost droplets, *Phys. Rev. Lett.*, 2006, **96**(15), 154502, DOI: 10.1103/PhysRevLett.96.154502.
9 G. Dupeux, M. Le Merrer, G. Lagubeau, C. Clanet, S. Hardt and D. Quéré, Viscous mechanism for Leidenfrost propulsion on a ratchet, *EPL*, 2011, **96**(5), 58001, DOI: 10.1209/0295-5075/96/58001.
10 T. R. Cousins, R. E. Goldstein, J. W. Jaworski and A. I. Pesci, A ratchet trap for Leidenfrost drops, *J. Fluid Mech.*, 2012, **696**, 215–227.
11 G. G. Wells, R. Ledesma-Aguilar, G. McHale and K. Sefiane, A sublimation heat engine, *Nat. Commun.*, 2015, **6**(1), 6390.
12 G. Dupeux, T. Baier, V. Bacot, S. Hardt, C. Clanet and D. Quéré, Self-propelling uneven Leidenfrost solids, *Phys. Fluids*, 2013, **25**(5), 051704, DOI: 10.1063/1.4807007.
13 F. Brochard, Motions of droplets on solid surfaces induced by chemical or thermal gradients, *Langmuir*, 1989, **5**(2), 432–438, DOI: 10.1021/la00086a025.
14 S. Mettu and M. K. Chaudhury, Motion of drops on a surface induced by thermal gradient and vibration, *Langmuir*, 2008, **24**(19), 10833–10837, DOI: 10.1021/la801380s.
15 Q. Dai, M. M. Khonsari, C. Shen, W. Huang and X. Wang, Thermocapillary migration of liquid droplets induced by a unidirectional thermal gradient, *Langmuir*, 2016, **32**(30), 7485–7492, DOI: 10.1021/acs.langmuir.6b01614.
16 B. Sobac, A. Rednikov, S. Dorbolo and P. Colinet, Self-propelled Leidenfrost drops on a thermal gradient: A theoretical study, *Phys. Fluids*, 2017, **29**(8), 082101, DOI: 10.1063/1.4990840.
17 J. C. Burton, A. L. Sharpe, R. C. A. van der Veen, A. Franco and S. R. Nagel, Geometry of the vapor layer under a Leidenfrost drop, *Phys. Rev. Lett.*, 2012, **109**(7), 074301, DOI: 10.1103/PhysRevLett.109.074301.
18 I. U. Vakarelski, N. A. Patankar, J. O. Marston, D. Y. C. Chan and S. T. Thoroddsen, Stabilization of Leidenfrost vapour layer by textured superhydrophobic surfaces, *Nature*, 2012, **489**, 274–277.